Reversible Inhibition of Murine Cytomegalovirus Replication by Gamma Interferon (IFN-) in Primary Macrophages Involves a Primed Type I IFN-Signaling Subnetwork for Full Establishment of an Immediate ...

Kropp, Kai A.; Robertson, Kevin A.; Sing, Garwin; Rodriguez-Martin, Sara; Blanc, Mathieu; Lacaze, Paul; Hassim, Muhamad F. B. Noor Hassim; Khondoker, Mizanur R.; Busche, Andreas; Dickinson, Paul; ...

Source / Izvornik: **Journal of Virology, 2011, 85, 10286 - 10299**

Journal article, Published version
Rad u časopisu, Objavljena verzija rada (izdavačev PDF)

https://doi.org/10.1128/JVI.00373-11

Permanent link / Trajna poveznica: https://urn.nsk.hr/urn:nbn:hr:184:796831

JOURNAL OF VIROLOGY, Oct. 2011, p. 10286–10299 Vol. 85, No. 19
0022-538X/11/$12.00 doi:10.1128/JVI.00373-11

Reversible Inhibition of Murine Cytomegalovirus Replication by Gamma Interferon (IFN-γ) in Primary Macrophages Involves a Primed Type I IFN-Signaling Subnetwork for Full Establishment of an Immediate-Early Antiviral State▽†

Kai A. Kropp,[1] Kevin A. Robertson,[1,2] Garwin Sing,[1] Sara Rodriguez-Martin,[1] Mathieu Blanc,[1] Paul Lacaze,[1] Muhamad F. B. Noor Hassim,[1] Mizanur R. Khondoker,[1]‡ Andreas Busche,[3] Paul Dickinson,[1,2] Thorsten Forster,[1,2] Birgit Strobl,[4] Mathias Mueller,[4] Stipan Jonjic,[5] Ana Angulo,[6] and Peter Ghazal[1,2]*

Division of Pathway Medicine and Centre of Infectious Diseases, University of Edinburgh, Edinburgh, United Kingdom[1]; Centre of Systems Biology at Edinburgh University, The King's Buildings, Edinburgh, United Kingdom[2]; Institute of Virology, Hannover Medical School, Hannover, Germany[3]; Institute of Animal Breeding and Genetics, Department for Biomedical Sciences, University of Veterinary Medicine Vienna, Vienna, Austria[4]; Department for Histology and Embryology, School of Medicine, University of Rijeka, Rijeka, Croatia[5]; and Institut d'Investigacions Biomèdiques August Pi i Sunyer, Barcelona, Spain[6]

Received 23 February 2011/Accepted 11 July 2011

Activated macrophages play a central role in controlling inflammatory responses to infection and are tightly regulated to rapidly mount responses to infectious challenge. Type I interferon (alpha/beta interferon [IFN-α/β]) and type II interferon (IFN-γ) play a crucial role in activating macrophages and subsequently restricting viral infections. Both types of IFNs signal through related but distinct signaling pathways, inducing a vast number of interferon-stimulated genes that are overlapping but distinguishable. The exact mechanism by which IFNs, particularly IFN-γ, inhibit DNA viruses such as cytomegalovirus (CMV) is still not fully understood. Here, we investigate the antiviral state developed in macrophages upon reversible inhibition of murine CMV by IFN-γ. On the basis of molecular profiling of the reversible inhibition, we identify a significant contribution of a restricted type I IFN subnetwork linked with IFN-γ activation. Genetic knockout of the type I-signaling pathway, in the context of IFN-γ stimulation, revealed an essential requirement for a primed type I-signaling process in developing a full refractory state in macrophages. A minimal transient induction of IFN-β upon macrophage activation with IFN-γ is also detectable. In dose and kinetic viral replication inhibition experiments with IFN-γ, the establishment of an antiviral effect is demonstrated to occur within the first hours of infection. We show that the inhibitory mechanisms at these very early times involve a blockade of the viral major immediate-early promoter activity. Altogether our results show that a primed type I IFN subnetwork contributes to an immediate-early antiviral state induced by type II IFN activation of macrophages, with a potential further amplification loop contributed by transient induction of IFN-β.

Murine cytomegalovirus (MCMV) infection in mice is a well-established model system for the study of acute, persistent, and latent infections of betaherpesviruses and their control by the host immune system (32, 35, 58, 60). Both human CMV (HCMV) and MCMV infect a broad range of tissues in their respective hosts, including fibroblasts, endothelial and epithelial cells, and, significantly, immune cells of the myeloid lineage (13, 57, 69, 70). Differentiated macrophages of this lineage residing in infected tissues play a key role in eliciting the host immune response but are also permissive for CMV infection and serve as disseminators of the virus throughout the host (reviewed in reference 29).

In immunocompetent hosts, primary CMV infections are generally asymptomatic, with immune cells either killing virus-infected cells or restricting viral cell-to-cell spread and replication. The latter effect occurs via induction of an antiviral state in noninfected cells or the activation of immune cells by soluble mediators such as type I interferon (alpha/beta interferon [IFN-α/β]) and type II interferon (IFN-γ) (8, 10, 41, 50, 60, 73). Several hundred genes stimulated in response to both type I and type II IFNs have been identified by microarrays in various cell types over the years (18, 19, 37, 38, 66). In contrast, the recently discovered type III IFNs are not well characterized but may have comparable functions to the type I IFNs, mediated by shared downstream signaling and IFN-stimulated genes (ISGs) (3, 33, 42, 63, 72, 78, 84). Type III IFNs are

* Corresponding author. Mailing address: Division of Pathway Medicine, University of Edinburgh Medical School, The Chancellor's Building, 49 Little France Crescent, Edinburgh EH16 4SB, United Kingdom. Phone: 44 131 242 6284. Fax: 44 131 242 6244. E-mail: P.Ghazal@ed.ac.uk.

† Supplemental material for this article may be found at http://jvi.asm.org/.

‡ Present address: Department of Biostatistics, Institute of Psychiatry and NIHR Biomedical Research Centre for Mental Health at the South London and Maudsley NHS Foundation Trust, King's College London, London, United Kingdom.

▽ Published ahead of print on 20 July 2011.

predominantly expressed in epithelial cells (72), and in this regard, activated murine bone marrow-derived macrophages (BMDMs) showed no induction of type III expression in our cell system (P. Ghazal, P. Lacaze, and K. A. Robertson, unpublished data). Historically, IFN-α and IFN-β have been closely associated with induction of an antiviral state affecting RNA viruses, while DNA viruses have proven more susceptible to IFN-γ regulation, which also has an important role in homeostasis of immune-modulatory functions. The different types of IFNs bind to their cognate receptors, which activate mainly distinct but related Janus kinase/signal transducers and activators of transcription (JAK/STAT)-signaling cascades, resulting in the rapid induction of gene transcription (11, 74). These distinctions have become increasingly blurred over the years by reports of overlapping downstream signaling events and cross talk between the type I-, II-, and III-signaling pathways (25, 52, 55, 67, 68, 78, 85), demonstrating that the different types of IFNs do not act absolutely independently.

IFNs suppress viral replication by activating a vast number of cellular processes with direct and indirect antiviral effects which render the cell less permissive for viral replication (40, 45, 63). Therefore, determining the precise mechanisms of viral inhibition by ISGs remains problematic, due to a pleiotropic response. In the case of MCMV infection, it has been demonstrated that IFN-γ plays a crucial role in modulating the immune response to infection (6, 30, 31) and in controlling persistently replicating virus (60). It is known, for example, that IFN-γ pretreatment induces an antiviral state in NIH 3T3 fibroblasts by blocking the activity of the major immediate-early (MIE) promoter (MIEP) (26, 50). Recently, it has been shown that pretreatment of mouse embryonic fibroblasts (MEFs) (85) or BMDMs (61) with IFN-γ also directly establishes an antiviral state in these cell types. So far the mechanisms underlying this block of MCMV replication in bone marrow-derived macrophages are not fully understood. It is notable, however, that the prototypic antiviral effector proteins, such as Mx1, RNase L, or protein kinase R (PKR), do not seem to play a role in this response, as BMDMs from the respective knockout (KO) mice were still protected by IFN-γ treatment. Interestingly, in the study of Presti et al., this effect seemed to be independent of type I signaling, as IFN-αR1$^{-/-}$ BMDMs pretreated with IFN-γ showed no significant increase in permissiveness compared to the control cultures (61).

In more recent studies, we have investigated the changes in the BMDM transcriptome after type II IFN stimulation combined with targeted RNA interference (RNAi) knockdown in whole-genome microarray experiments (44) and found that an interferon regulatory factor (IRF)/type I IFN transcriptional network plays an important role in stimulating ISGs following IFN-γ treatment. However, the question of whether a full type I IFN transcriptional network or subnetwork plays a role in eliciting an antiviral state in BMDMs after type II IFN stimulation is not clear.

In the present work, we further characterize the type II-induced antiviral state in BMDMs using a reversible inhibition approach and now provide evidence for the identification of a type I IFN subnetwork contributing significantly to the rapid shutdown of the major immediate-early promoter activity and establishment of the refractory state in IFN-γ-pretreated BMDMs in the context of MCMV infection.

MATERIALS AND METHODS

Mice. BALB/c and C57BL/6 (BL6) mice were purchased from Charles River Laboratories (Kent, United Kingdom) and maintained under specific-pathogen-free conditions at the University of Edinburgh. Housing and animal procedures were approved by the United Kingdom Government Home Office. If not indicated differently, BL6 BMDMs have been used for the experiments. Mouse strains C57BL/6 IFN-αR1$^{-/-}$, Tyk2$^{-/-}$, and IFN-β1$^{-/-}$ were maintained under specific-pathogen-free conditions at the Institute of Animal Breeding and Genetics, Department for Biomedical Sciences, University of Veterinary Medicine Vienna, Vienna, Austria. The generation or source of knockout mouse strains for IFN-αR1$^{-/-}$, Tyk2$^{-/-}$, and IFN-β1$^{-/-}$ has been described elsewhere (see references 21 and 76 and references therein).

Cells and viruses. Macrophage cultures were established from the bone marrow of 10- to 12-week-old male mice as described previously (15, 44). Briefly, bone marrow progenitors were flushed from femurs and tibias and plated in tissue culture dishes (Costar; Corning Inc., NY). The cells were cultured in Dulbecco modified Eagle medium–Ham F-12 medium-glutaMAX medium supplemented with 10% fetal calf serum (FCS), 50 U/ml penicillin and streptomycin, and 10% L929 conditioned medium as a source of macrophage colony-stimulating factor (referred to as BMDM growth medium in this report). At 6 days postisolation, cells had differentiated into mature macrophages, as assessed by surface expression of Mac-1 and F4/80 markers, and had reached approximately 80% confluence.

MEFs derived from the embryos of timed pregnant C57BL/6 mice on days 14 to 17 of gestation were cultured in Eagle's minimum essential medium (EMEM) supplemented with 10% FCS, 50 U/ml penicillin and streptomycin, and 2 mM glutamine. MEFs were used at passage 3 postisolation for experiments.

The bacterial artificial chromosome (BAC)-derived MCMV strain pSM3fr (81) (designated MCMV in this report) was used as wild-type (WT) virus.

The *Gaussia* luciferase (GLuc) reporter virus (GLuc-MCMV) was generated by site-specific homologous recombination (12, 54, 81). Shortly, the GLuc open reading frame (ORF), amplified with primers 5′-GCGTCTAGAGCCGGCgacg tcgaagagaacccgggcccgATGGGAGTCAAAGTTCTGTTTG-3′ and 5′-CTCGAT ATCTTAGTCACCACCGGCCCCCTTGAT-3′ from plasmid pCMV-GLuc (New England BioLabs), was cloned into pMCMV3 (12, 14), resulting in pmMIEP-GLuc. The mCherry ORF amplified with primers 5′-GCGAAGCTTAT GCATGCCGCCATGGTGAGCAAGGGCGAGGA-3′ and 5′-GTCGCCGGC ctgcttcaggaggctgaagttcgtggctcccgagccCTTGTACAGCTCGTCCAT-3′ from the template pCMVBrainbow1.1 (49) was inserted into pmMIEP-GLuc, resulting in pmCherryP2AGLuc. Each of the primer sequences in lowercase letters encodes one-half of the picornaviral 2A amino acid sequence. Finally, a kanamycin resistance marker flanked by FLP recombination target sites (12) was inserted, leading to pmCherryP2AGLucKanR. MCMV BACs were mutated by homologous recombination in *Escherichia coli* using the mutagenesis procedure as described previously (12). Briefly, PCR fragments were generated using plasmid pmCherryP2AGLucKanR, and the primers 5′-AATCTGAACCCCGATATTT GAGAAAGTGTACCCCGATATTCAGTACCTCTTCAGGAACACTTAAC GGCTGA-3′ and 5′-ACCCGGGCCCTTCACGGTAAGGATCTGACAGTCG ACCGTCGATTCGTCAGTTTGAATTCGAGCTCGCCCAACTCCG-3′. The 50 nucleotides (nt) at the 5′ ends of the primers were required for homologous recombination with the m157 sequence in the MCMV BAC. The PCR product was electroporated into *E. coli* containing the BAC pSM3fr (81). Recombined BACs were characterized by restriction analysis. The kanamycin resistance marker was subsequently excised by FLP recombinase (12).

For the fluorescent infection assays, BMDMs were infected with a recombinant reporter virus expressing the green fluorescent protein (GFP) marker, under the control of the HCMV enhancer/promoter, inserted into exon 1 of the *ie2* gene (pSM3fr-rev, called GFP-MCMV in this report and described in detail elsewhere [1]).

For production of viral stocks, virus strains were propagated on mouse NIH 3T3 cells (ATCC CRL1658) and stocks were prepared as described previously (58).

IFN-γ treatment and virus infections. To analyze reversible induction of the antiviral state by IFN-γ, macrophage cultures were treated with recombinant mouse IFN-γ (biological activity, 9.4×10^3 U per μg; RM200120; Thermo Scientific) as follows: (i) untreated (−IFN-γ), in which BMDMs were differentiated for 8 days and subsequently used for experiments; (ii) pretreated (+IFN-γ), in which, on day 7 postculture, cells were prestimulated with 10 U/ml IFN-γ (Genetech, Oceanside, CA) for 24 h, after which the medium was removed and

fresh BMDM growth medium was added; and (iii) pretreated and withdrawn (w-IFN-γ), in which, on day 6 postculture, cells were treated with 10 U/ml IFN-γ for 24 h. On day 7, the IFN-γ was removed, and the cells were washed briefly in medium to remove residual cytokine and incubated in fresh BMDM growth medium for 24 h. On day 8, cells were used for experiments.

For replication assays in IFN-treated cells or other procedures, BMDMs were treated on day 6 with 10 U/ml IFN-γ, if not stated differently, and subsequently infected as follows.

Infections were basically done as described elsewhere (47). Briefly, infection was carried out in ~10 to 20% of the initial culture volume, and concentrated virus suspension was added to achieve a multiplicity of infection (MOI) of 1. Cells were incubated with viral particles for an adsorption period of 1 h at 37°C and then washed 3 times with phosphate-buffered saline (PBS). Fresh medium was added, and cells were further incubated as indicated in the respective experiment.

For viral replication assays, 10% of the total supernatant volume from respective 6-well cultures was harvested at the indicated time points, and the culture was replenished with an equal volume of fresh medium. Samples were either stored at −80°C or analyzed immediately on permissive MEFs by standard plaque assay (47).

Fluorescent virus infectivity assays. For analysis of reporter expression in GFP-MCMV-infected BMDMs, cells were analyzed by flow cytometry. BMDMs were isolated and cultured as described above. On day 5 postisolation, BMDMs were scraped off and transferred into 24-well tissue culture plates (2×10^5 cells/well). On day 6, BMDMs were pretreated with IFN-γ for 24 h and subsequently infected (GFP-MCMV; MOI, 1). At 6 h postinfection (p.i.), samples were scraped off, pelleted by centrifugation, and resuspended in 350 μl buffer (PBS, 1% bovine serum albumin, 1 mM sodium azide).

The prepared samples were analyzed using a Becton Dickinson FACsCalibur machine (BD Biosciences, Oxford, United Kingdom) and Cellquest Pro software, gathering 1×10^4 detection events (excitation, 488 ± 10 nm; detection filter, 530 nm). Additional data analysis was conducted using Flowjo (version 9.2) software (Tree Star Inc., Ashland, OR). In all experiments, WT MCMV-infected BMDMs were used to control for background signal levels produced by autofluorescence of infected BMDMs.

GLuc reporter assay. To measure viral replication or MIEP activity in cells infected with GLuc-MCMV, BMDMs were pretreated as described and cells were infected with an MOI of 1. GLuc is efficiently secreted in mammalian cell systems (82), so cell culture supernatants were harvested and frozen (−20°C) at the indicated time points for later analysis. GLuc activity was measured using the native form of the GLuc substrate coelenterazine (C-7001; Biosynth, Staad, Switzerland). Coelenterazine was dissolved in nitrogen-saturated acidified methanol (with 0.1 M HCl) to prepare a stock solution (10 mM) (80). Coelenterazine work solution (20 nM) was freshly produced by diluting 50 μl stock solution 1:500 in PBS–5 M NaCl (nitrogen saturated) and incubating the solution for 30 min with protection from light. Enzyme activity was measured with a POLARstar plate reader (BMG Labtech, Offenburg, Germany) in well mode, injecting 50 μl coelenterazine work solution per well and integrating the light signal over a measurement period of 20 s. Signal intensities of the wells were normalized to values at 1 s postinjection.

(i) Replication assay. To measure viral replication by GLuc activity, BMDMs were seeded in 100 μl medium (96-well format) and differentiated for 6 days. Cells were pretreated as described above and infected on day 8. At the indicated time points, 15 μl of culture supernatant was repeatedly harvested and replaced with fresh medium. Subsequently, 10 μl of the samples was used to measure enzyme activity.

(ii) Synthesis assay. To analyze MIEP activity, BMDMS were prepared as described above (96-well format) and infected. At the indicated time points, cell culture supernatant of infected BMDMs was completely removed (100 μl) and replenished with fresh medium. Subsequently, MIEP activity was then analyzed by measuring enzyme activity in 50 μl supernatant.

Real-time reverse transcription-PCR (RT-PCR). To measure the expression levels of viral immediate-early (IE) genes, the GFP gene, or host candidate genes, BMDMs were differentiated for 6 days. Cells were treated as described above and infected (MOI, 1). Total cellular RNA was isolated at 6 h postinfection (RNeasy minikit; Qiagen, Hilden, Germany), quality controlled, and transcribed into cDNA using an anchored poly(T) primer (Transcriptor first-strand cDNA synthesis kit; Roche Diagnostics, Burgess Hill, United Kingdom). DNA templates were diluted 1:10, and changes in viral gene expression levels were analyzed by relative quantitative real-time PCR using TaqMan primers and probe combinations as described elsewhere (43, 51). Ready-to-use probe/primer sets were used to analyze tumor necrosis factor alpha (TNF-α) and glyceraldehyde-3-phosphate dehydrogenase (GAPDH) transcript levels (TaqMan gene expression assay; Applied Biosystems, Carlsbad, CA) as described elsewhere (44), and PCRs for detecting viral genes were carried out using HotStar *Taq* (Qiagen) as recommended by the manufacturer, except for increasing the $MgCl_2$ concentration to 2.5 mM.

Host candidate genes were detected using the Roche Universal Probe Library (UPL). Gene-specific probe/primer combinations were designed using the Roche Assay Design Center web application (the UPL probes and primers used in this study are detailed in Table S5 in the supplemental material).

ET_{50}. The half-maximum (50%) effective pretreatment time (ET_{50}) is basically identical to the half-maximum (50%) effective or inhibitory concentration (EC_{50} and IC_{50}, respectively) used to describe the efficiency of inhibitory drugs. Therefore, ET_{50} was determined by using an online tool designed to calculate EC_{50}s (BiodataFit, version 1.02; Chang Bioscience). Viral titers of pretreated and control BMDM cultures and pretreatment times ($n = 3$) were used to calculate ET_{50} values with a best-fit model.

Gene expression profiling. Total cellular RNA was isolated as described previously (15, 44). Briefly, BMDMs were lysed with TRIzol (Invitrogen, CA) and the RNA was prepared according to the manufacturer's instructions. Sample concentration and purity were measured by spectrophotometry, and RNA integrity was monitored using an Agilent 2100 bioanalyzer system (Agilent, Palo Alto, CA). Five micrograms of total RNA was converted into double-stranded cDNA that was then used as a template for T7 RNA polymerase *in vitro* transcription in the presence of biotinylated ribonucleotides (Enzo Diagnostics). All procedures were followed according to the manufacturer's instructions (Affymetrix, Santa Clara, CA). Fifteen micrograms of each biotinylated cRNA was fragmented and hybridized to Affymetrix MG-U74Av2 Genechip microarrays for 18 h and then washed and scanned using a Agilent 2500A scanner according to the standard protocol. Microarray images were processed using Affymetrix Microarray Analysis Suite (version 5.0) software.

Microarray data processing and statistical analysis. The numerical data were processed and analyzed with the Bioconductor package for the R statistical programming environment (62). Raw data distributions and summary statistics were assessed for quality. Using the robust multichip average (RMA) algorithm (36), data were then corrected for background, quantile normalized, and probe set summarized. Null hypotheses for each gene were based on the comparison between mock arrays and each of the biological conditions (three independent biological replicates for each condition) and were tested using an empirical Bayes moderated *t* test (71). The false discovery rate associated with simultaneous testing of multiple genes was controlled using the Benjamini-Hochberg *P* value adjustment method (5). Genes were interpreted on the basis of differential expression between the mock-infected group and each of the two experimental groups and the corresponding statistical significance. Annotations and functional classification of gene elements were derived from the Affymetrix NetAffx analysis center. For cluster analysis of array data, BioLayout Express 3d (23) was used with a Pearson correlation cutoff of ≥0.95. To map interferon-induced genes with the Interferome database (described in reference 64; available at http://www.interferome.org/search.php), Affymetrix identifiers (IDs) were annotated to EMBL IDs by using the clone/ID converter (http://idconverter.bioinfo.cnio.es/) online tool. Functional network and pathway analysis was carried out with the Ingenuity application (IPA; Ingenuity Systems Inc.) using the fold changes and *P* values derived from the statistical analysis described above. IPA dynamically generates networks of gene, protein, small-molecule, drug, and disease associations on the basis of hand-curated data held in a proprietary database. To enhance the explorative interpretation of data, networks are ranked according to a score calculated via a right-tailed Fisher's exact test. This test outputs a value that takes into account the original input gene or proteins of interest and the size of the network generated. The value enables the application to approximate how relevant the network is to the analysis. Further information on the computational methods implemented in IPA can be obtained from Ingenuity Systems Inc.

Microarray data accession number. All microarray data are publicly available online in the GPX database (http://gpxmea.gti.ed.ac.uk/), microarray data accession number GPX-00002911, or made available as stated in the respective references.

RESULTS

Dose and time dependency of the IFN-γ-induced antiviral state. To characterize the antiviral effects of IFN-γ in our primary BMDM system, we assessed the effect of pretreatment time on the inhibition of viral replication for IFN-γ concentrations of 1, 10, and 100 U/ml (Fig. 1A). These experiments

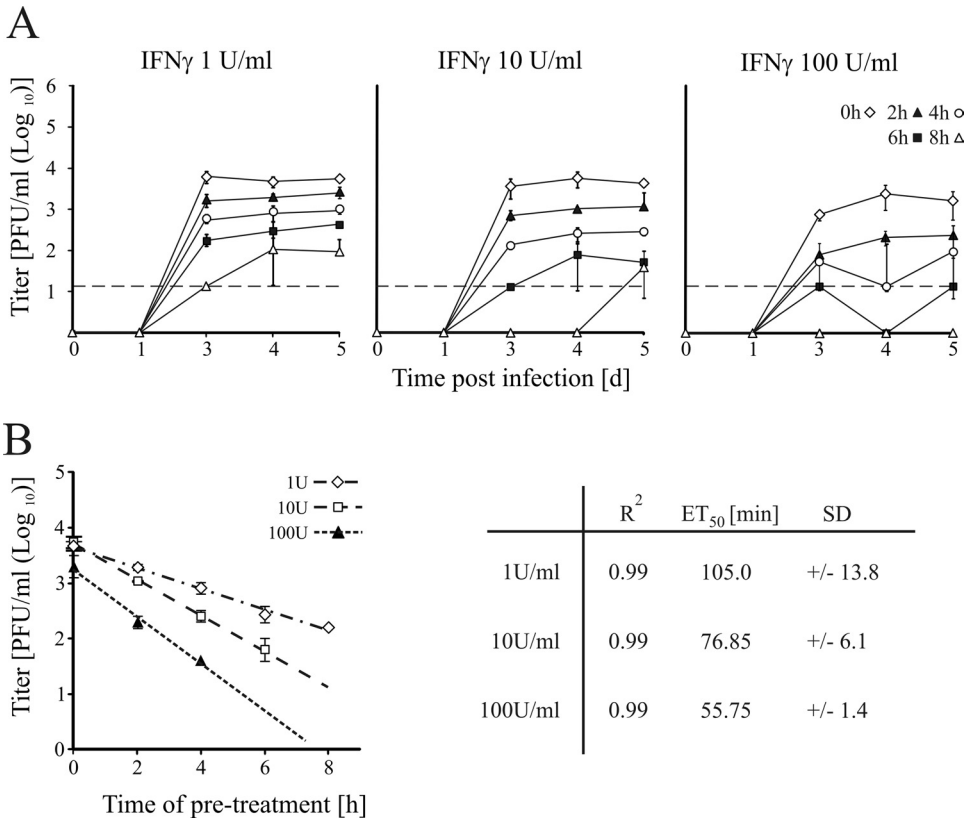

	R^2	ET_{50} [min]	SD
1U/ml	0.99	105.0	+/- 13.8
10U/ml	0.99	76.85	+/- 6.1
100U/ml	0.99	55.75	+/- 1.4

FIG. 1. Dose and time dependency of the IFN-γ-induced antiviral state. (A) Viral replication was measured by plaque assay in BMDMs that were pretreated for 2 h, 4 h, 6 h, or 8 h with IFN-γ or left untreated (0 h) before infection with MCMV (MOI, 1). Cells were pretreated with 1, 10, or 100 U/ml IFN-γ, as indicated. Dashed lines represent detection limits. Data points located on the *x* axis represent cultures without detected plaques; data points on the dashed line indicate cultures with single infection events. If not stated differently, in this and all subsequent figures, data points depict averages ($n = 3$) and error bars represent SDs. d, days. (B) Correlation of pretreatment time and antiviral effect. Plot of pretreatment times against viral titers on day 4 showed a log-linear correlation ($R^2 = 0.99$) for all three IFN-γ concentrations (1 U/ml, 10 U/ml, and 100 U/ml). ET_{50}s were calculated by a best-fit model for comparison of plaque numbers of the respective pretreated samples with pretreatment time.

show that pretreatment of BMDMs with IFN-γ reduces virus production in replication assays and that virus production shows a strong dependency on the timing of pretreatment. For all three concentrations, a pretreatment time of 2 h triggered a measurable reduction in the numbers of released viral particles throughout the complete replication assay (Fig. 1A). This antiviral effect was further enhanced with longer pretreatment times (4, 6, and 8 h). Incubation with IFN-γ for 8 h was sufficient to establish a complete inhibition of viral replication with 10 and 100 U/ml IFN-γ, while pretreatment for 6 h suppressed viral replication efficiently so that only a single plaque developed with 100 U/ml at days 3 and 5 p.i. However, with 10 U/ml IFN and 8 h pretreatment, we could observe a recovery of replication at day 5, indicating that with this particular concentration of IFN, the antiviral effect was not sustained for prolonged incubation periods. Plotting the $\log_{10}$ of the viral titers at day 4 against the pretreatment time revealed an inverse log-linear correlation between viral titers and pretreatment time, with R^2 values being ≥0.99 (Fig. 1B). Most notably, we observed an effective inhibition with all tested IFN-γ concentrations with a pretreatment of less than 2 h. To more accurately quantify this effect, we determined the ET_{50}s using a best-fit model of the data shown in Fig. 1B. This analysis estimated ET_{50}s of 105 min (±13.8 min), 76.85 min (±6.1 min), and 55.75 min (±1.4 min) for 1, 10, and 100 U/ml, respectively.

From these experiments we conclude that there is a direct correlation between pretreatment times with IFN-γ and the antiviral effect in BMDMs. The detectable lag phase and calculated ET_{50} values indicate that the inhibitory effect most likely requires cellular factors that change over time after the initial stimulus. We also note that the antiviral state is effective within the first hour of IFN-γ treatment. In this connection, it is noteworthy that pretreatment with IFN-γ does not affect viral entry (61; P. Ghazal and M. F. Hassim, unpublished observation).

The antiviral effects of IFN-γ are dependent on persistent stimulation. The apparent loss of antiviral activity at late times after a single treatment is consistent with the well-established observation that a continuous stimulation with IFN-γ is necessary for accumulation of IFN-γ-induced gene products (22, 24). Therefore, to further assess whether the continuous presence of IFN-γ is required to efficiently block viral replication in our experimental system, different cultures of BMDMs were either continuously or transiently stimulated with IFN-γ for 24 h. Cells were transiently stimulated by incubation with IFN-γ for 24 h, followed

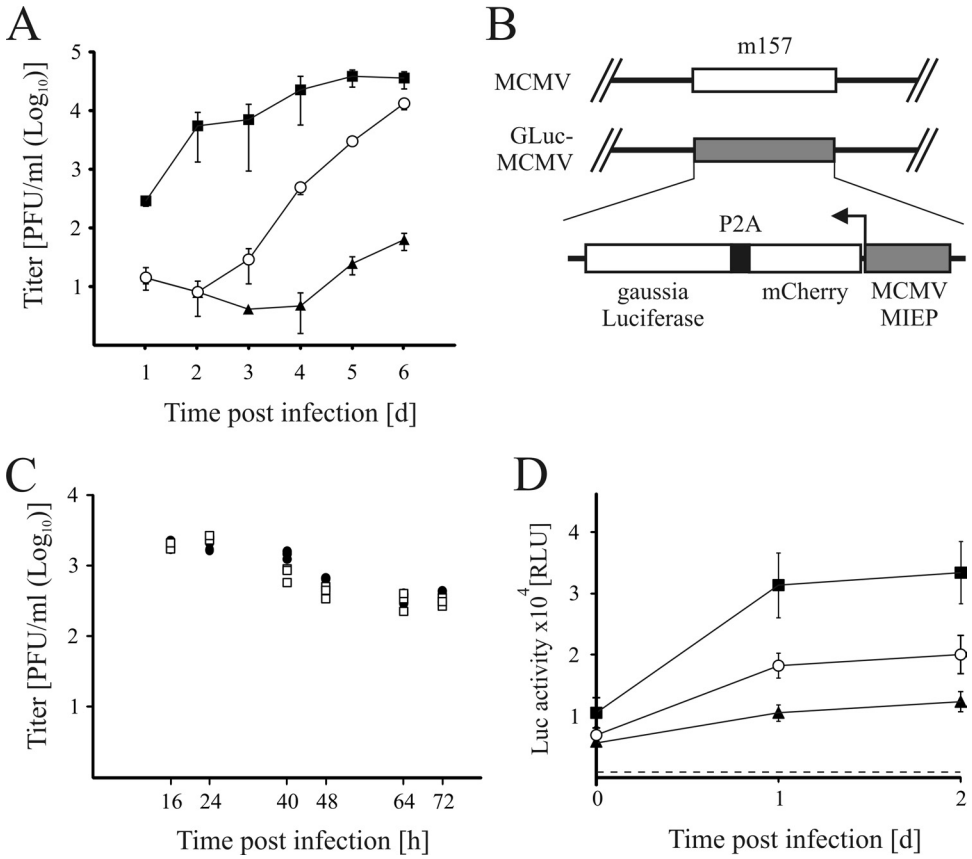

FIG. 2. The antiviral effects of IFN-γ are dependent on persistent stimulation. BMDMs were continuously treated with 10 U/ml IFN-γ (+IFN-γ; black triangles) or transiently treated (w-IFN-γ; white circles) or were left untreated (−IFN-γ; black squares); cells were subsequently infected (MOI, 1). (A) The IFN-γ-induced antiviral state is reversible. BMDMs were pretreated as described and infected at time point 0 with MCMV. Culture supernatant was analyzed on primary MEFs for secreted infectious virus until the plateau phase for the untreated control was reached. (B) Schematic representation of the m157 region in wild-type MCMV and mutant reporter virus strain GLuc-MCMV. Reporter gene expression in the mutant strain is controlled by an additional MCMV MIEP element. Both reporter genes are expressed as one bicistronic mRNA and autocatalytically cleaved during the translation process by peptide 2A of the foot-and-mouth-disease virus. (C) Replication of both virus strains in BMDMs is comparable. Viral replication of MCMV (black circles) and GLuc-MCMV (white squares) in BMDMs was measured by standard plaque assay on primary MEFs and is indistinguishable for both virus strains. (D) Effects of 10 U/ml IFN-γ pretreatment on viral replication of GLuc-MCMV are already evident in the first 48 h after infection. Viral replication was monitored by repeated measurement of extracellular levels of *Gaussia* luciferase in 10 μl culture supernatant. Data points represent means (n = 10; error bars are SDs), and the dashed line indicates the level of the background signal. Symbols are as described for panel A.

by an additional 24-h period in normal medium prior to infection. As shown in Fig. 2A, the inhibition of the viral replication induced by the 24-h IFN-γ pretreatment gradually diminished following removal of the cytokine stimulus. Although the replication kinetics of the virus infecting the rested cells were delayed by about 48 h compared to viral growth kinetics in untreated cells, virus yield gradually increased to levels comparable to those for nontreated cells by 6 days postinfection. In contrast, infected cells cultured in the continuous presence of IFN-γ showed a persistent suppression of CMV replication (Fig. 2A). This demonstrates that the IFN-γ-mediated inhibition of viral replication is reversible upon withdrawal of the stimulus.

Since the inhibitory effect is detectable at very early times (Fig. 1B) and the measurement by plaque assays is not amenable or sensitive enough for detecting early replication kinetics, we next sought to investigate whether reversible inhibition by IFN-γ affects the very early stages of viral replication. For the purpose of these experiments, we used a quantitatively more sensitive *Gaussia* luciferase reporter virus (GLuc-MCMV) replication assay. In the newly constructed GLuc-MCMV, the reporter gene is controlled by the MIEP element of MCMV and can be utilized to determine early replication kinetics (Fig. 2B). Importantly, as shown in Fig. 2C, GLuc-MCMV replication is comparable to that of MCMV in BMDMs. Accordingly, we used reporter virus infection of pretreated BMDMs to assess the effects of IFN-γ on the early phase of replication. In contrast to the results of the plaque assay, infecting BMDMs with GLuc-MCMV in the presence of IFN-γ led to a reduced reporter gene expression during the first 48 h of infection that was partially reversed after removal of IFN-γ (Fig. 2D). The results of these experiments reveal that the IFN-γ-induced blockage of viral replication can also occur at a very early phase of the infection. As has been speculated by others (61), this could be caused by a block in MIEP activity.

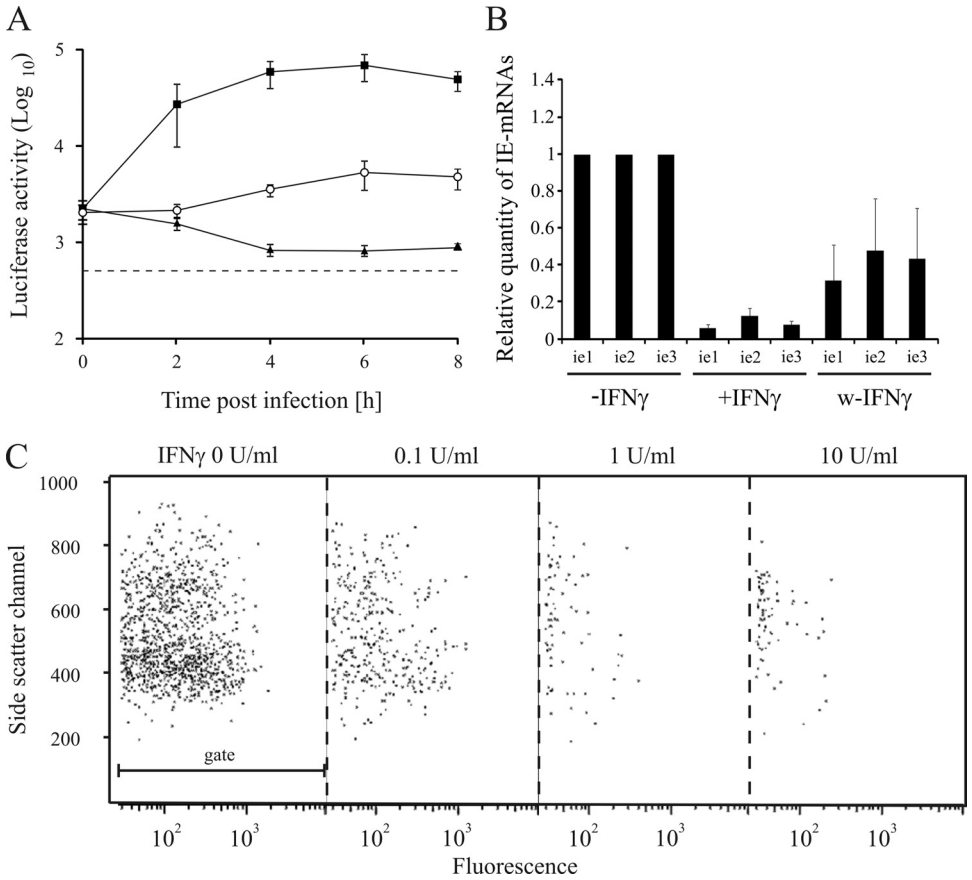

FIG. 3. Establishing an antiviral state in BMDMs involves a blockage of MIEP activity. (A) The inhibitory effect of IFN-γ is already evident in the immediate-early phase of viral replication. MIEP activity was measured by GLuc synthesis assay. BMDMs that were continuously treated with 10 U/ml IFN-γ (+IFN-γ; black triangles), transiently treated (w-IFN-γ; white circles), or untreated (−IFN-γ; black squares) were infected with GLuc-MCMV (MOI, 1). GLuc activity released into cell culture supernatant was measured in 2-h time windows, and supernatant was completely replaced at each indicated sampling point. Data points represent means (n = 6; error bars are SDs), with the dashed line indicating the level of the background signal. (B) IFN-γ treatment reversibly inhibits expression of the viral major IE genes. Relative comparison of mRNA levels of MIE genes by quantitative real-time PCR. BMDMs were pretreated and infected as described for panel A. Total cell cDNA was analyzed with intron-spanning MIE gene-specific TaqMan probes and compared to that from untreated samples. Cellular GAPDH mRNA was used for normalization. Bars represent mean relative quantification values of 3 independent biological replicates (error bars depict SEMs). (C) Measurement of reporter expression in individual cells. Flow cytometry side scatter and GFP fluorescence dot plots of GFP-positive gated BMDM populations (dot plots of complete populations are available in Fig. S4 in the supplemental material). Cells pretreated with the indicated IFN-γ concentrations for 24 h and subsequently infected (MOI, 1) with GFP-MCMV were harvested at 6 h p.i., and 10,000 cells for respective treatments were analyzed for GFP expression. Autofluorescence of BMDMs infected with MCMV was used to define the threshold for the GFP gate.

Induction of the antiviral state in BMDMs involves a blockade of MIEP activity. In the initial report of an IFN-γ-induced antiviral state in BMDMs by Presti et al. (61), a reduction in IE1 protein and mRNA levels in IFN-γ-treated cells which was not attributable to differences in the amount of virus uptake was demonstrated. Significantly, however, it is not known whether a reduced promoter activity or a specifically targeted degradation of viral transcripts is responsible for the antiviral phenotype. With this in mind and to further investigate whether the IE phase of viral infection is susceptible to IFN-γ control, we analyzed the GLuc expression during the immediate-early and early phases of the infection cycle. In these experiments, BMDMs were infected with GLuc-MCMV (MOI, 1) and GLuc activity in the culture was measured for the first 8 h p.i. Figure 3A shows strongly reduced reporter gene expression in the IFN-γ-treated cultures. In agreement with the reporter gene expression in the replication assay (Fig. 2D), we detected increased reporter gene levels in cultures that were rested for 24 h after removing IFN-γ. The levels of GLuc activity in the rested cultures did not reach the levels of the mock-treated culture, supporting the proposed partial relief of the blockage.

It is possible that the reporter system used in these assays does not represent the endogenous MIEP activity. To determine if the measurement of the reduced reporter gene levels in our system accurately reflects MIEP activity, we concurrently measured the endogenous viral major immediate early (MIE) gene expression in GLuc-MCMV-infected cells. In these experiments, we compared mRNA levels of the viral MIE transcripts by relative quantitative two-step RT-PCR between the different conditions (Fig. 3B). Oligo(dT) primers were used to produce cDNA from polyadenylated transcripts, and the cellular marker gene GAPDH was used to normalize expression levels of viral MIE gene transcripts. Notably, viral *ie1*, *ie2*, and *ie3* cDNAs were less abundant in

IFN-γ-treated cells than in rested cells. This observation was in concordance with the previously observed reversible blockade of reporter gene expression.

To control if the observed effects on viral MIEP and reporter gene expression are restricted to the GLuc-MCMV system, we used a second, distinct reporter virus (1) carrying the GFP gene under the control of the functionally homologous HCMV enhancer/promoter (2) inserted into the first exon of the *ie2* gene in the MCMV genome (GFP-MCMV). We analyzed the effects of three IFN-γ concentrations (0.1, 1, and 10 U/ml) on IE1, IE3, and GFP mRNA levels by quantitative RT-PCR (qRT-PCR) (see Fig. S1 in the supplemental material). The levels of IE mRNAs were quantitatively reduced to a similar extent as the GFP mRNA. The observed reduction in GFP expression also demonstrates that the inhibitory effects of IFN-γ are not restricted to the GLuc reporter virus. The fact that the genetic locus carrying the reporter genes differs among the different reporter viruses further indicates that the reduced expression levels are not caused by any position-related effects and that the MIEP blockage is not acting exclusively on the MCMV enhancer but also affects the HCMV enhancer.

The reporter gene assays and the analysis of the transcript levels described above indicate that the pretreatment with IFN-γ reduces MIEP activity in BMDMs. Significantly, both assays yield an ensemble measurement of the cell culture samples. In other words, these experiments represent an average measurement of the entire population of cells and do not distinguish between a general population effect and a potential reduction in only a subset of the population of infected cells.

For this reason, we next sought to analyze the cell frequency distribution of MIEP activity in our cell culture system using the GFP-tagged reporter virus (1). Pretreated BMDMs were infected, and GFP levels in the infected cells were measured by flow cytometry. This assay shows a strong reduction in the number of GFP-positive cells as well as a drop in the number of highly fluorescent cells, as demonstrated by the dot plots of GFP fluorescence level per cell of the gated population (Fig. 3C).

Altogether these experiments provide multiple lines of evidence showing that pretreatment with IFN-γ induces a blockade of viral replication which is already evident at the level of MIEP activity. Moreover, the different reporter and endogenous mRNA expression assays demonstrate that the antiviral mechanism is not specifically targeting the MIE mRNAs of MCMV but does influence the activity of the MIE promoter/enhancer element controlling the expression of the essential viral MIE gene locus.

It is also noteworthy that these results further indicate that the IFN-γ-inhibitory effect of MCMV in BMDMs involves partially reversible inhibition of the MIEP activity and viral replication, suggesting that both nonreversibly and reversibly stimulated cellular factors (ISGs) can influence the IFN-γ-induced antiviral state.

Analysis of gene transcript profiles in BMDMs reversibly treated with IFN-γ and identification of candidate genes underlying the reversible antiviral state in BMDMs. As the antiviral state is partially reversible, we assume that cellular gene products involved in establishing this state are regulated correspondingly. Thus, to investigate the cellular changes associated with the reversible and the nonreversible refractory state, we performed microarray analysis (GPX accession number for data set, GPX-000029.1) of cellular gene expression levels in IFN-γ-pretreated BMDMs and BMDMs after IFN-γ withdrawal. In these experiments, total RNA samples were labeled and hybridized to murine genome MG-U74Av2 arrays (Affymetrix). Approximately 50% of the total number of probes present on the arrays fulfilled these criteria and were considered detected in the experiment: 6,231 (mock treated), 5,903 (+IFN-γ), and 6,081 (w-IFN-γ) probes produced a detectable signal with the indicated samples.

For the purpose of this investigation, we first focused our analysis on genes whose expression is differentially upregulated by IFN-γ treatment (i.e., ISGs). On this basis, a comparison of the +24-h IFN-γ data set with the mock-treated control identified 521 targets that were strongly induced (the full gene list is available in Table S1 in the supplemental material). This is in good accordance with the 511 IFN-γ-induced genes reported by others (37). Next, the 521 identified IFN-stimulated probe set was further subjected to cluster analysis with BioLayout Express3d. Using a Pearson correlation cutoff of 0.95 produced 5 clusters of coregulated genes (Fig. 4A), with 33 targets having values below the cutoff and 18 targets being excluded from further analysis due to incomplete annotation. Clusters 1 and 2 contain 405 genes that are induced by IFN-γ and seemed to return to the baseline level of expression in the samples when IFN-γ was withdrawn (Fig. 4A, blue-shaded clusters); clusters 3 and 4 contain 49 genes that were induced but maintained an elevated expression level after IFN-γ withdrawal (red-shaded clusters). The last cluster consists of 16 genes that were induced by IFN-γ and showed no reduction in expression levels (green cluster) in the samples after withdrawal of IFN-γ (w-IFN-γ). As shown in Fig. 2 and Fig. 3, the IFN-γ-induced antiviral state in BMDMs is partially reversible by removing IFN-γ from the culture. Under these reversible conditions, underlying candidate genes would be expected to be expressed correspondingly. To more precisely identify candidate genes in the groups for the reversible and the nonreversible phenotypes, we applied a more stringent statistical testing (eBayes test, with $P < 0.05$), comparing expression levels in the w-IFN-γ samples with those in the mock-treated samples and accepting only targets for the reversible phenotype that were not significantly upregulated in the w-IFN-γ samples in comparison to the mock-treated samples. This analysis identified 163 targets (group A in Fig. 4B) that were induced compared to the mock-treated control in the +24-h IFN-γ data set but showed no significant difference between the mock treatment and the w-IFN-γ data sets. This demonstrates that this group of genes is dependent on a continuous stimulation with IFN-γ for regulation. In contrast to this, 358 genes (group B) showed an elevated expression level compared to that for the mock treatment after withdrawal of IFN-γ and therefore formed the group of candidate genes for the nonreversible component of the MIEP blockage.

To identify canonical pathways and functional networks in these groups, we used the Ingenuity pathway analysis tool. The analysis emphasized the pleiotropic cellular response to IFN-γ treatment, with ~200 canonical pathways and 65 functional networks being associated with the IFN-γ-induced genes. As expected, we found high correlations between our input genes

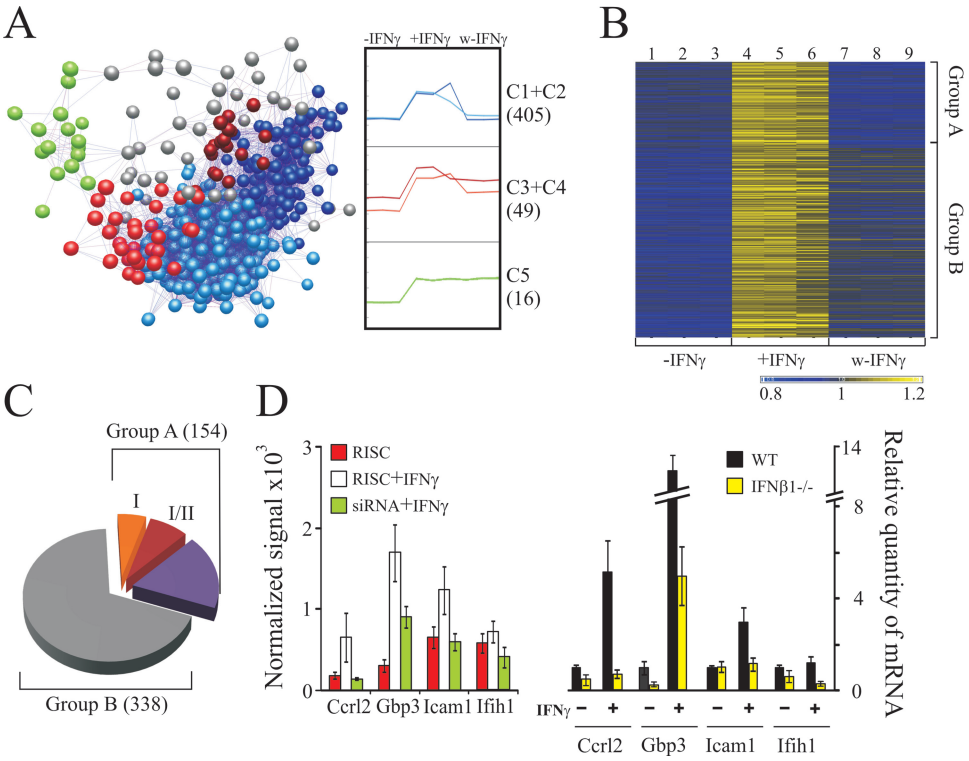

FIG. 4. Analysis of gene transcription profiles in BMDMs treated with IFN-γ. BMDMs (BALB/c) were treated with IFN-γ (3 replicates) as described (+IFN-γ or w-IFN-γ) or left untreated (−IFN-γ). Statistical analysis of the array data (GPX accession number GPX-000029.1) then identified 521 probes whose expression was significantly altered. (A) Cluster analysis of the 521 identified targets. Expression profiles of the 521 targets over the three conditions were compared, and a Pearson correlation of 0.95 was used as the cutoff for cluster formation. Profiles grouped into five clusters (clusters C1 to C5), indicated in the corresponding line plots, which show the average expression profile of the corresponding clusters over the three conditions (right). Gene numbers in the groups are shown in parentheses. In the network representation of the clustering (A), gray nodes represent 33 probe sets that were below the cutoff for clustering, and 18 probes were excluded due to incomplete annotation. (B) Heat map of the 521 identified targets with three replicates for each condition (continuously numbered). Expression levels were normalized to the average of the data set. Statistical testing (empirical Bayes test) was used to filter for genes that reversed expression levels completely after withdrawal of IFN-γ. One hundred sixty-three targets which fulfilled the criteria were identified ($P \leq 0.05$). The heat map was produced using supervised clustering, which organized 163 targets into group A and the remaining 358 targets into group B. (C) Type I IFN-induced genes form a substantial part of the induced transcriptional network. Probe sets were mapped to a nonredundant list of ENSEMBL identifiers, resulting in 492 discrete candidates for further analysis. This list was used to query the Interferome database to identify genes specifically induced by type I IFNs. For the 154 ENSEMBL identifiers from group A, 27 genes were specifically induced by type I IFNs (I), 38 genes were induced by type I or type II IFNs (I/II), and 89 genes could not be mapped to the database. (D) IFN-β influences basal and induced expression levels of candidate host genes in the IFN-γ BMDM system. Genes of group A were compared to array data from BMDMs transfected with control siRNAs (RISC) or an siRNA targeting IFN-β and subsequently treated with IFN-γ (44). (Left) Average microarray expression data ($n = 3$) for five exemplary target genes; (right) qRT-PCR data for the same set of genes in WT and IFN-$\beta 1^{-/-}$ BMDMs after treatment with 10 U/ml IFN-γ. A complete list of target genes and expression levels for the microarray and qRT-PCR data set are available (see Table S3 and Fig. S2 in the supplemental material).

and networks related to the inflammatory response, antigen presentation, cellular development, and cell signaling. Notably, networks related to cellular movement, cell-to-cell signaling and interactions, cell death, lipid metabolism, and molecular transport were also found to be associated with our candidate genes (summarized in Table S4 in the supplemental material). In this connection, we have recently shown that genes involved in sterol biosynthesis contribute to the antiviral state at late times of infection, showing that continuous exposure to IFN-γ is necessary to sustain the reduction in cholesterol biosynthesis (9). Significantly, we found that most networks had members drawn from both the reversible and nonreversible gene sets. Notably, however, some networks, e.g., the functional network for antigen presentation, had a stronger correlation with genes that maintained an elevated expression level (49 common genes; $P < 6.5 \times 10^{-11}$), while the functional network for gene expression was stronger correlated to the reversibly induced genes (48 common genes; $P < 9.1 \times 10^{-10}$).

This microarray analysis provides candidate gene lists and functional networks for the mechanistic analysis of the IFN-γ-induced antiviral effect in BMDMs. A more in-depth analysis and functional systematic screening of candidate genes will be undertaken in future investigations.

Type I IFN-responsive genes constitute a part of the IFN-γ-induced transcriptional changes in BMDMs. In the various gene sets associated with the reversible inhibition, there is a striking type I IFN-related component detectable. Analysis of the 163 transiently induced targets identified a group of candidates that have been described to be induced specifically by type I signaling (18), i.e., *Mx1/2*, *Ifit2* (*IFI-54K*), *Ifih1* (*MDA-5*), and *Ifitm3* (48). Furthermore, comparison of the group of 163 transiently induced candidate genes (group A) with the se-

quences in the Interferome database (64) showed a significant number of genes (Fig. 4C) that have been demonstrated to be specifically induced by type I IFNs (27 of 65 mapped genes) or by both type I and type II IFNs (38 of 65 mapped genes), while 89 genes of group A could not be mapped to the database (a summary of the analysis is provided in Table S2 in the supplemental material). Although a significantly smaller number of the 358 genes could be mapped to sequences in the Interferome database, the analysis of the mapped genes of group B gave comparable results (see Table S2 in the supplemental material).

IFN-β influences the expression levels of the induced candidate genes. The fact that we observed the expression of genes that are typically induced by type I IFNs raised the question of whether the expression of these genes represented an overlap between the type I and type II responses or whether there might be a more direct functional involvement of type I IFN signaling. We therefore assessed if the type I-signaling pathway is directly involved in the IFN-γ-induced phenotype in our experimental system. As shown in Fig. 2, the antiviral effects of IFN-γ pretreatment are reversible and, therefore, dependent on a continuous stimulation with IFN-γ. Figure 4A and B demonstrates that the 163 targets in group A show a dependency on IFN-γ for the maintenance of their expression profiles. To extend our understanding of type I IFN-signaling in this system, we compared the expression levels of our 163 induced targets with those from a microarray data set from our previous study (44). Data from a representative group of these genes is presented in Fig. 4D, left (the full data set is available in Table S3 in the supplemental material). In BMDMs with a small interfering RNA (siRNA)-mediated knockdown of IFN-β, more than 50% of the targets identified in our study showed reduced expression levels compared to cells treated with a control siRNA (RNA-induced silencing complex [RISC] free) after stimulation with IFN-γ. These results indicate that the induction of the target genes by IFN-γ is dependent on IFN-β expression. Next, we extended the comparison of our 163 targets to STAT1 and STAT2 knockdown experiments (44) and found comparable results.

The above study points to either a priming of BMDM cultures by type I IFNs or an increased expression due to the induction of an autocrine IFN-β feedback loop. To further evaluate the involvement of IFN-β, we next measured the relative expression levels of selected candidate genes in IFN-γ-treated BMDMs from WT and IFN-β1$^{-/-}$ mice by qRT-PCR (Fig. 4D, right; the full data set is available in Fig. S2 in the supplemental material). In these experiments, most of the tested candidate genes showed an already reduced expression level in IFN-β1$^{-/-}$ mock-treated cultures, supportive for a priming of BMDM cultures by type I IFNs. In addition to this, expression levels of the candidate genes were also less responsive to IFN-γ treatment in IFN-β1$^{-/-}$ cells than WT cells. Altogether these experiments suggest that approximately 50% of our candidate gene list is dependent on a primed type I IFN signaling, potentially with an additional inducible amplifier feedback loop.

Type I IFNs play a functional role in establishing the IFN-γ-induced antiviral state. Analysis of the data obtained so far indicated a contribution of the type I IFN system to the establishment of the type II-induced antiviral state in BMDMs that is most likely due to a priming effect of the type I IFN-signaling pathway. However, the question of whether an IFN-γ stimulus directly induces type I IFN expression in our system remains open.

In order to examine this question, we first considered from microarray experiments changes in IFN-β expression levels in BMDMs treated with IFN-γ over a period of 12 h (9). This analysis showed a transient and relatively small, ~4-fold, increase in IFN-β expression between 4 h and 6 h after the stimulus (Fig. 5A). Notably, we did not detect any changes in expression levels of several members of the IFN-α gene family or IFN-ζ (see Fig. S3 in the supplemental material). Probes detecting type III interferons were not present on this array, but in other microarray studies, we found no detectable increase of abundance of type III IFNs (interleukin-28a/b; K. A. Robertson and P. Ghazal, unpublished observation). To explore whether this increase in RNA levels was accompanied by a measurable increase in levels of secreted IFN-β, we proceeded to analyze cell culture supernatants from IFN-γ-treated BMDMs using an IFN-β-specific enzyme-linked immunosorbent assay (ELISA). As shown in Fig. 5B, we were able to detect small amounts of IFN-β in the cell cultures, with levels rising to 40 pg/ml from 6 h after IFN-γ treatment, just at the limit of detection of our assay. The increase is slightly delayed from the increase in RNA levels, which is to be expected. In contrast to this observation, infected control cultures produced up to 1,000 pg/ml IFN-β (data not shown). This result indicates the possibility that a potential autocrine amplifier loop cannot be excluded from contributing to the antiviral state by transient induction of IFN-β.

Ability of IFN-γ to inhibit release of viral particles is affected by impaired type I IFN signaling. To clarify if the type I IFNs contribute to the antiviral state in direct functional assays, we used systems with impaired type I IFN-signaling pathways for further analysis. In experiments to test if type I signaling plays a role in the inhibition of MCMV replication, we analyzed viral infection of BMDMs derived from homozygous genetic IFN-αR1$^{-/-}$ and Tyk2$^{-/-}$ mice and compared this with infection of WT BMDMs on days 3 and 5 postinfection. The number of infectious particles in a cell culture supernatant of infected BMDMs was measured by standard plaque assay on MEFs. It is known that BMDMs of type I-KO mice are more susceptible for MCMV replication (76); therefore, ratios between IFN-γ-pretreated and untreated cultures were calculated to allow comparison between the different KO systems. Relative efficiencies of plaque formation were calculated by comparing mean values for plaque numbers in the IFN-γ-treated samples with those in the respective mock-treated BMDMs for each genetic background at each time point (Fig. 5C).

It has been proposed that type I receptors colocalize with type II receptors, and therefore, the deletion of IFN-αR1 could impair type II signaling by influencing receptor dimerization (77). To control for this, we included BMDMs from Tyk2$^{-/-}$ mice in our analysis. In these cells, IFN-αR1 levels are comparable to those in WT BMDMs (39), but downstream signaling events of the type I IFN signaling are reduced. Pretreatment of BMDMs from both types of knockout mice with IFN-γ reduced the efficiency of plaque formation to a lesser extent than in wild-type BMDMs,

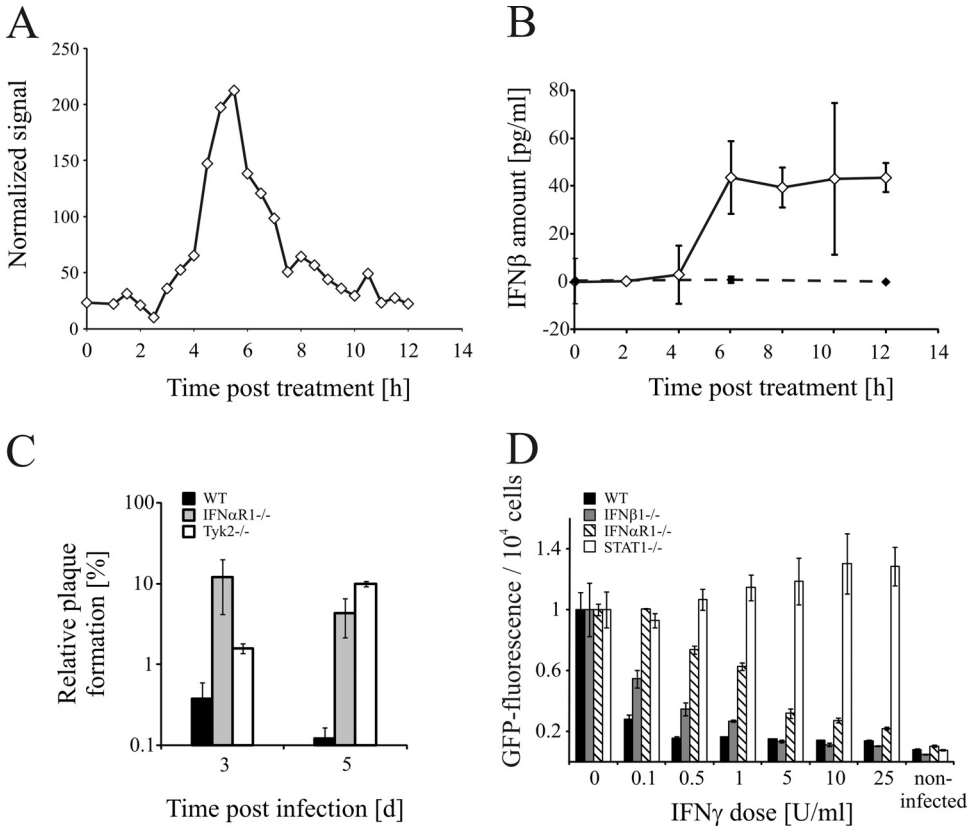

FIG. 5. Type I IFNs play a functional role in establishing the IFN-γ-induced antiviral state. (A) Low levels of IFN-β mRNA transcription are induced by IFN-γ stimulation. Normalized IFN-β expression levels were derived from an Agilent V2 array with cDNA from IFN-γ-treated BMDMs (BALB/c). Total cellular RNA was sampled at the indicated time points, and the derived cDNA was analyzed by whole-genome microarray, as described in reference 9. (B) Minimal IFN-β secretion is induced in IFN-γ-treated cells. The concentration of IFN-β in supernatants of IFN-γ (10 U/ml)-treated BMDM cultures from BALB/c mice was measured by ELISA (white rhombs). Supernatant from mock-treated cultures was used as a negative control (black rhombs). (C) Type I IFNs contribute to the IFN-γ-induced antiviral state in BMDMs. Plaque assay measuring viral replication in BMDMs pretreated with IFN-γ. BMDMs from wild type, IFN-αR1$^{-/-}$, or Tyk2$^{-/-}$ mice were pretreated with 10 U/ml IFN-γ and infected with MCMV (MOI, 1). Relative plaque formation was calculated at each indicated time point from means of treated and untreated samples. Error bars depict SDs of the ratios. We used the delta method (17) as an approximation to obtain an error estimate for the calculated ratio of treated over untreated. The estimate is calculated under the assumption that the two variables are normally distributed, independent, and not correlated. (D) Type I IFNs contribute to the IFN-γ-induced block of viral IE gene expression. BMDMs from wild type, IFN-β1$^{-/-}$, IFN-αR1$^{-/-}$, or STAT1$^{-/-}$ mice were pretreated with IFN-γ and subsequently infected with GFP-MCMV (MOI, 1). Cells were fixed at 6 h p.i. and analyzed by flow cytometry for GFP expression.

demonstrating that IFN-αR1 and the downstream type I signaling are necessary to fully establish an antiviral state by IFN-γ treatment.

The block of MIEP activity is reduced in BMDMs with impaired IFN signaling. Our analysis of IFN-γ effects on reporter gene expression suggests that a part of the mechanism of IFN-γ-induced antiviral activity involved a blockade of MIEP activity (Fig. 3). To investigate if the functionality of the type I-signaling pathway is necessary for this blockade, we analyzed normalized GFP reporter gene expression in BMDMs derived from IFN-αR1$^{-/-}$, IFN-β1$^{-/-}$, and STAT1$^{-/-}$ mice. As shown in Fig. 5D, dose-dependent inhibition of GFP expression by IFN-γ and, therefore, MIEP activity showed an absolute dependency on STAT1 and a partial dependency on type I signaling. Deletion of the type I receptor IFN-αR1 had a strong effect, leading to higher levels of GFP than in wild-type BMDMs after IFN-γ pretreatment and infection. Significantly, deletion of the IFN-β1 gene also increased the GFP expression, demonstrating that the contribution of type I IFNs to the MIEP blockage is dependent on IFN secretion and is not restricted to a cytoplasmic cross talk between the type I and type II-signaling pathways alone. However, inhibition by IFN-γ is less effective in the IFN-αR1$^{-/-}$ BMDMs than the IFN-β1$^{-/-}$ BMDMs. It is likely that members of the IFN-α gene family also play a role and can partially compensate for the loss of IFN-β. Furthermore, the difference in GFP levels between WT BMDMs and the type I-deficient BMDMs was smaller for higher IFN-γ concentrations, indicating that high doses of IFN-γ can compensate for a loss of type I signaling. Overall, the above work demonstrates that the involvement of type I IFNs is necessary for the establishment of a full IFN-γ-induced blockade of MIEP activity. Further, when low, arguably physiologically more relevant doses of IFN-γ were analyzed, we found that small quantities of type I IFNs are sufficient to develop a full IFN-γ-induced antiviral response.

DISCUSSION

In this paper we have investigated the antiviral effects of IFN-γ on the MCMV transcription-replication cycle in primary BMDMs. We demonstrate that the IFN-γ effect is a rapidly initiated process within the first hour of stimulus exposure that increases during the first 8 h of pretreatment and is triggered by doses of IFN-γ as low as 1 U/ml. The antiviral effects of IFN-γ may be reversed by resting cells for 24 h after the removal of IFN-γ. This raises the notion of a select temporal window for effective control of infection by IFN-γ, with important implications for *in vivo* acute and latent infections. Mechanistically, we further demonstrate that pretreatment of BMDMs with IFN-γ alters the level of MIE gene transcription controlled by the MIEP. Finally, we identified clusters of cellular candidate genes of potential importance to the above observations by analyzing their expression profiles and found that the type I IFN-signaling pathway is functionally important to the antiviral effects of IFN-γ.

It is now well established that IFN-γ is an important antiviral factor which controls *in vivo* MCMV replication and disease (7, 31, 41, 60, 73). More recently, it was described that the pretreatment of primary cells, i.e., BMDMs and MEFs, with IFN-γ renders these cell types less susceptible to MCMV infection. This effect was stronger in BMDMs than in MEFs, was absolutely dependent on STAT1 function, and proved to be independent of the genes for the cellular effectors PKR, RNase L, and inducible nitric oxide synthase. Notably, in the study of Presti et al. (61), the signaling molecules TNF-α and type I IFNs (IFN-α/β) did not play a significant role in eliciting the antiviral effect in BMDMs derived from the corresponding receptor-knockout mice. From a mechanistic perspective, the IFN-γ pretreatment of BMDMs led to reduced levels of viral ie1, e1, m54, and gB mRNAs and IE1 and E1 protein levels (61). In accordance with this report, we now show that IFN-γ pretreatment directly affects the transcriptional activity of the MIEP. We are aware that this represents only a part of the whole multifactorial IFN-γ antiviral response. In this connection, we have recently shown that IFN-γ-mediated inhibition of MCMV replication in BMDMs involves the reduction of the sterol biosynthesis pathway (9) at later times of infection (initiated at 6 h p.i., with a maximal effect at 24 h p.i.).

It is well-known that the IFN-γ effect involves induction of gene transcription and protein synthesis, and our results indicate that the antiviral state involves rapidly induced transcription of cellular factors that are active at as early as 1 to 2 h posttreatment and accumulate during the next few hours. We have described the very early effects (within the first hour) of IFN-γ stimulation on NIH 3T3 cells (20). In this regard, others have also reported IFN-γ-mediated inhibition of MCMV in NIH 3T3 fibroblasts at very early times of infection. However, this was associated with reduced MIE gene transcription by high doses of IFN-α or IFN-γ (1,000 inhibitory units/ml) in reporter plasmids (26) and was reported to be due to down-regulation of NF-κB (27). However, the role for NF-κB in inhibition or activation of the viral MIEP in infected cultures is controversial (4, 28).

A similar observation has also been made in BMDMs, where inhibition of the virus was associated with reduced levels of IE1 and E1 mRNA and protein (61). In this study, we confirmed these findings in BMDMs and added further evidence for a blockade of viral promoter activity comparable to reported IFN-γ effects in the NIH 3T3 fibroblast system. Significantly, a quantitative real-time PCR analysis of MIE mRNA levels in IFN-γ-treated cultures demonstrated that these transcripts were reduced in abundance compared to mock-treated cultures. The use of different reporter viruses demonstrated, furthermore, that this effect was most likely caused by a reduced MIEP activity and not by a sequence-specific degradation of viral MIEP mRNAs by, e.g., antiviral host micro-RNAs (46, 65). This demonstrates that in BMDMs, the refractory state is associated with a reduced expression of the essential viral MIE genes, which are crucial to the initiation of the viral replication cycle (1, 53).

We have further demonstrated, for the first time, a reversible IFN-γ-induced blockade of the viral transcription-replication cycle. Significantly, our results show that the reversible phenotype coincides with a restoration of MIEP activity. Notably, however, in contrast to the plaque numbers, the MIEP activity showed only a partial recovery. In relation to this observation, it has recently been described that reduced MIEP activity is sufficient to sustain viral replication *in vitro* and *in vivo* (43, 59). This observation could explain our observed differences in the levels of inhibition between MIEP activity and release of viral particles, where reduced MIEP activity appears to be sufficient to maintain viral replication in our system. These results raise the possibility that the blockage of MIEP activity is multifactorial and may comprise a component whose activity is independent of continuous IFN-γ stimulation and another component whose activity is reversible and dependent on the continuous presence of IFN-γ.

Alongside its ability to directly block viral replication, IFN-γ also plays an important role as a link between the innate and adaptive immune responses (8, 11, 67). It has been demonstrated that the innate immune response is capable of limiting CMV during the first week of infection. Significantly, however, without a functional adaptive immune response, the virus eventually overcomes this control (31, 50, 56). The reversible block of MIEP activity described here may provide a temporal window of opportunity for CMV to escape the innate immune response when levels of IFN activity drop.

IFNs induce a pleiotropic response in cells and upregulate the expression of hundreds of genes (18, 19, 37). In this study, we have exploited a reversible IFN-γ-induced refractory state to identify candidate genes with potential antiviral functions at early times of infection. We applied a pathway analysis of the nonreversibly and reversibly induced genes for enrichment of functional networks. In the group of the reversibly induced host factors, we found an enrichment of networks strongly associated with regulators of the IFN pathway, signaling molecules, as well as some effector genes. Notably, analysis of the candidate genes identified a group of genes that have been described to be exclusively IFN type I specific (18, 48).

Type I IFNs are known to effectively inhibit MCMV replication in NIH 3T3 cells and BMDMs (26, 76). It is noteworthy that in our study we did not observe a prototypic type I response involving antiviral factors such as PKR, RNase L, ISG-15, or oligoadenylate synthetase. This is in agreement with the study of Presti and colleagues, where corresponding cells from knockout mice showed no significant differences in permissive-

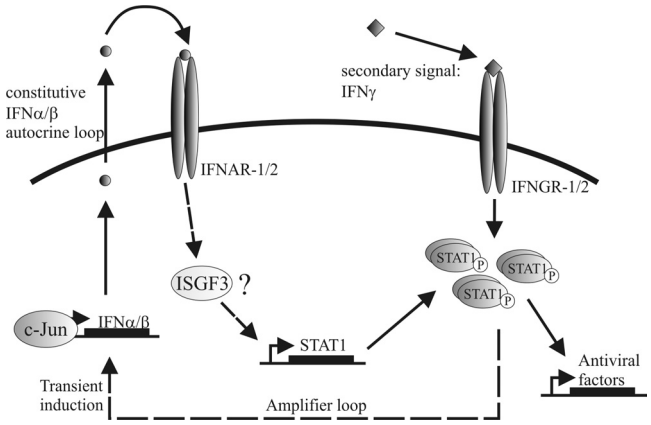

FIG. 6. Schematic model of the cross talk between type I and type II signaling. The constitutive subthreshold expression of type I IFNs is mediated by c-Jun binding to the IFN-β enhancer (25) but is not triggering a full-scale type I response. Binding of subthreshold levels of type I IFNs by their cognitive receptor leads to low-level expression of type I-stimulated genes and is necessary to maintain expression levels of STAT1. A functional role for STAT2 in this system has been demonstrated (85), although it is not clear if ISGF3 is involved in the constitutive autocrine loop. Type I signaling mainly functions through ISGF3 activation but can also directly activate STAT1 homodimers, which in turn could induce expression of the STAT1 gene. This primes cells for the secondary IFN-γ signal, increasing sensitivity for extracellular IFN-γ levels. The IFN-γ signal then induces the expression of several hundred target genes, establishing an antiviral state. Some of the induced genes, namely, MDA-5, TBK1, TANK, IRF1, IRF7, and IRF8, are components of IFN-β-inducing pathways, therefore probably facilitating the observed transient expression of IFN-β by IFN-γ. This transient induction provides an additional feedback loop in the system, temporarily amplifying the constitutive autocrine loop and probably further increasing the levels of STAT1. If the functionality of the constitutive type I autocrine loop is impaired, levels of STAT1 are reduced and the system will be less responsive to the secondary IFN-γ signal.

ness (61). Instead, we identified a type I subnetwork consisting of upregulated members of the tripartite motif (TRIM) family, Ifit2 (ISG-54K), Ifih1 (MDA-5), and Ifitm3. In addition, we detected small quantities of transiently induced IFN-β protein in cultures at about 6 h after treatment with IFN-γ. These results are somewhat contradictory to a report from Costa-Pereira and colleagues (16), who found no induction of type I IFNs by IFN-γ. Significantly, however, in that study, human U5A cells were used and the divergent results probably reflect differences between experimental systems. In support of this conclusion, others have reported the induction of type I IFNs by IFN-γ in mouse macrophages (83).

Notably, analysis of expression levels of host candidate genes in IFN-β1$^{-/-}$ cells by qRT-PCR demonstrated that these genes were dependent on type I IFNs either to maintain their basal expression levels or to fully respond to the IFN-γ stimulus. Taken together, this demonstrates that priming of cells with a potential restricted autocrine type I IFN loop plays an important role in establishing the antiviral effects of IFN-γ (Fig. 3D and schematically shown in Fig. 6).

In agreement with this, we observed in this study the induction of MDA-5, TANK, TBK1, STAT1, IFN-αR2, IRF1, IRF8, and IRF7 in IFN-γ-treated samples. These are factors typically involved in type I-signaling cascades (34) and would, therefore, increase the sensitivity of the type I amplifier loop as well as prime the system for other type I IFN-inducing factors. Our current results and prior siRNA-knockdown studies demonstrate that the IFN-γ-induced antiviral state in BMDMs is not independent of IFN type I activity and that disruption of IFN-β expression or function reduces the effects of IFN-γ. These results seemingly contradict those from the study of Presti et al. (61), who found no dependence of IFN-γ-mediated effects on type I IFNs in IFN-αR1$^{-/-}$ BMDMs. However, it is notable that Presti and colleagues used 100 U/ml of IFN-γ for 48 h to pretreat BMDMs (61). As we have demonstrated in this study, the dependence on type I IFNs becomes especially relevant at low concentrations of IFN-γ (lower than 10 U/ml) because higher IFN-γ levels seem to compensate for the loss of the type I function. Therefore, our results do not necessarily contradict those from the study of Presti et al. (61) but extend their findings to lower and presumably more physiological concentrations of IFN-γ.

Interestingly, in our gene expression experiments we found no induction of other type I IFNs, although IFN-α transcripts were detectable at low levels at all time points but did not increase in abundance following IFN-γ stimulation. Interestingly, IFN-λ cytokines have their own set of receptors but share downstream signaling elements with type I IFNs, inducing a type I-like response (42, 78, 84). In this regard, we note that a recent publication demonstrated that IFN-λ production is cell specific and that this cytokine acts predominantly on epithelial cells (72). The array platform that we used contained no probes directed against type III IFNs; however, we did not detect any differential expression of type III IFNs in other microarray experiments in our cell system (Robertson and Ghazal, unpublished).

Despite the fact that we could not detect expression of the typical type I-induced antiviral factors discussed above, we did find a substantial contribution of the type I-signaling network to the IFN-γ-induced refractory state. This raises the question of how the type I IFN-signaling network can influence the IFN-γ effect, when only minute amounts are transiently induced in the system by IFN-γ alone.

It has become clear in the last few years that the IFN-signaling pathways do not function independently and that cross talk occurs between their constituent components (25, 52, 55, 67, 68, 78). One of the molecular mechanisms underlying this is the priming of cells for type II stimuli by small amounts of type I cytokines. This model was first described following work in an encephalomyocarditis virus (EMCV) infection system (77, 79). In this system, it has been demonstrated that type I IFN signaling and constitutive subthreshold expression of type I IFNs are necessary to mount a full protective IFN-γ response in pretreated cells (Fig. 6). Further, IFN-β constitutively expressed prior to any stimulation with IFN-γ has been shown to be necessary to maintain STAT1 levels for IFN-αR1 blockage by antibodies, and it has been shown that depletion of IFN-β reduces STAT1 levels (25). In agreement with those studies, reduced STAT1 and STAT2 levels have been reported in IFN-αR1$^{-/-}$ and Tyk2$^{-/-}$ BMDMs (39, 75, 76). Furthermore, in the study by Zimmermann et al. (2005), it was shown that IFN-α/β contributes to an IFN-γ-induced refractory state in MEFs and that MCMV counteracts this mechanism through the virus-encoded factor M27. This viral protein triggers the

degradation of STAT2, a component of the ISGF3 complex and an element of the type I-signaling cascade (85).

In the work presented here, we provide evidence that a functional type I-signaling pathway is essential for establishing a full antiviral state in IFN-γ-treated BMDMs and that the contribution of type I IFNs is necessary for this mechanism. In this regard, it is notable that the amount of IFN-β that was induced by pretreatment with IFN-γ alone is small compared to the amount of IFN-β induced by the infection process itself. Further, we could not detect a full type I response in IFN-γ-pretreated cells, indicating that the IFN-β concentration was below a threshold required to trigger a type I-induced antiviral state alone. These results suggest that the induced IFN-β in our system is unlikely to be directly triggering the antiviral state induced by IFN-γ. The possibility that the small amounts of IFN-β further amplify the constitutive priming levels of IFN type I in BMDMs is viable. We recognize, however, that the IFN-αR1$^{-/-}$, IFN-β1$^{-/-}$, and Tyk2$^{-/-}$ BMDMs used in this study do not allow us to completely determine the role of IFN-β in our system. The type I-deficient BMDMs have been shown to be more permissive for viral replication than WT BMDMs. It is therefore possible that the IFN-γ-induced effects are insufficient to complement the loss of a functional type I system at low levels. Furthermore, we cannot formally exclude the possibility that the inability to induce IFN-β after infection with MCMV is influencing the IFN-γ-induced phenotype. Significantly, however, we could still detect induction of an antiviral state in the type I-deficient BMDMs by IFN-γ.

Overall, the results reported here are consistent with the more recently refined EMCV model described above (25), although we do detect minute quantities of IFN-β in our system. However, these levels are unlikely to directly cause the antiviral state but could further amplify the sensitivity for an IFN-γ stimulus. In this scenario, a transient induction of IFN-β expression could increase STAT1 levels further and by that counteract desensitization of the system by induced inhibitors of STAT activity (see the model in Fig. 6).

In the *in vivo* context, this mechanism probably contributes significantly to the protective effects of IFNs for noninfected bystander cells close to a focus of CMV infection or reactivation. In support of this, we demonstrated that type I signaling is more important at low concentrations of IFN-γ. It is likely, therefore, that it would play a more significant role *in vivo*, where IFN-γ concentrations may occur at lower concentrations than applied in our *in vitro* systems.

In summary, our findings demonstrate that type I IFNs make a vital contribution to an IFN-γ-induced block of viral replication in BMDMs and an early mechanism of this inhibition involves a blockade of MIEP activity. Overall, this study provides further insights into the molecular mechanism of functional cross talk between type I and type II IFNs in the MCMV-macrophage system.

ACKNOWLEDGMENTS

This work was supported by the Welcome Trust (WT066784/Z/02/Z) and by the BBSRC (R36269) and the BBSRC/EPSRC (BB/D019621/1) to P.G. The Centre for Systems Biology at Edinburgh is a Centre for Integrative Systems Biology (CISB) supported by the BBSRC and EPSRC. The RNAi Global Initiative provided reagent support for RNAi studies. K.A.K. is supported by the German Research Foundation (DFG; KR 3890/1-1), and B.S. and M.M. were funded by the Austrian Science Foundation FWF (SFB F28) and the Austrian Federal Ministry for Science and Research (GEN-AU III). A.B. is supported by SFB 587, project A13, and A.A. holds a grant from the Ministerio de Educación y Ciencia (SAF2008-00382).

We thank Martin Messerle for his helpful discussions and critical reading of the manuscript.

REFERENCES

1. **Angulo, A., P. Ghazal, and M. Messerle.** 2000. The major immediate-early gene ie3 of mouse cytomegalovirus is essential for viral growth. J. Virol. **74:**11129–11136.
2. **Angulo, A., M. Messerle, U. H. Koszinowski, and P. Ghazal.** 1998. Enhancer requirement for murine cytomegalovirus growth and genetic complementation by the human cytomegalovirus enhancer. J. Virol. **72:**8502–8509.
3. **Ank, N., et al.** 2006. Lambda interferon (IFN-{lambda}), a type III IFN, is induced by viruses and IFNs and displays potent antiviral activity against select virus infections in vivo. J. Virol. **80:**4501–4509.
4. **Benedict, C. A., et al.** 2004. Neutrality of the canonical NF-{kappa}B-dependent pathway for human and murine cytomegalovirus transcription and replication in vitro. J. Virol. **78:**741–750.
5. **Benjamini, Y., and Y. Hochberg.** 1995. Controlling the false discovery rate: a practical and powerful approach to multiple testing. J. R. Stat. Soc. B **57:**289–300.
6. **Beutler, B., K. Crozat, J. A. Koziol, and P. Georgel.** 2005. Genetic dissection of innate immunity to infection: the mouse cytomegalovirus model. Curr. Opin. Immunol. **17:**36–43.
7. **Beutler, B., et al.** 2005. Genetic analysis of innate resistance to mouse cytomegalovirus (MCMV). Brief. Funct. Genomic. Proteomic. **4:**203–213.
8. **Beutler, B., et al.** 2006. Genetic analysis of host resistance: Toll-like receptor signaling and immunity at large. Annu. Rev. Immunol. **24:**353–389.
9. **Blanc, M., et al.** 2011. Host defense against viral infection involves interferon mediated down-regulation of sterol biosynthesis. PLoS Biol. **9:**e1000598.
10. **Bodaghi, B., et al.** 1999. Role of IFN-+-induced indoleamine 2,3 dioxygenase and inducible nitric oxide synthase in the replication of human cytomegalovirus in retinal pigment epithelial cells. J. Immunol. **162:**957–964.
11. **Boehm, U., T. Klamp, M. Groot, and J. C. Howard.** 1997. Cellular responses to interferon-gamma. Annu. Rev. Immunol. **15:**749–795.
12. **Borst, E. M., C. Benkartek, and M. Messerle.** 2007. Use of bacterial artificial chromosomes in generating targeted mutations in human and mouse cytomegaloviruses, p. 1–30. *In* J. E. Coligan, B. Bierer, D. H. Margulies, E. M. Shevach, W. Strober, and R. Coico (ed.), Current protocols in immunology. John Wiley & Sons, Inc., New York, NY.
13. **Brautigam, A. R., F. J. Dutko, L. B. Olding, and M. B. A. Oldstone.** 1979. Pathogenesis of murine cytomegalovirus infection: the macrophage as a permissive cell for cytomegalovirus infection, replication and latency. J. Gen. Virol. **44:**349–359.
14. **Chatellard, et al.** 2007. The IE2 promoter/enhancer region from mouse CMV provides high levels of therapeutic protein expression in mammalian cells. Biotechnol. Bioeng. **96:**106–117.
15. **Cheung, G. Y. C., et al.** 2008. Transcriptional responses of murine macrophages to the adenylate cyclase toxin of Bordetella pertussis. Microb. Pathog. **44:**61–70.
16. **Costa-Pereira, A. P., et al.** 2002. The antiviral response to gamma interferon. J. Virol. **76:**9060–9068.
17. **Cox, C.** 1990. Fieller's theorem, the likelihood and the delta method. Biometrics **46:**709–718.
18. **Der, S. D., A. Zhou, B. R. G. Williams, and R. H. Silverman.** 1998. Identification of genes differentially regulated by interferon alpha, beta, or gamma using oligonucleotide arrays. Proc. Natl. Acad. Sci. U. S. A. **95:**15623–15628.
19. **de Veer, M. J., et al.** 2001. Functional classification of interferon-stimulated genes identified using microarrays. J. Leukoc. Biol. **69:**912–920.
20. **Doelken, L., et al.** 2008. High-resolution gene expression profiling for simultaneous kinetic parameter analysis of RNA synthesis and decay. RNA **14:**1959–1972.
21. **Erlandsson, L., et al.** 1998. Interferon-[beta] is required for interferon-[alpha] production in mouse fibroblasts. Curr. Biol. **8:**223–226.
22. **Fan, X. D., M. Goldberg, and B. R. Bloom.** 1988. Interferon-gamma-induced transcriptional activation is mediated by protein kinase C. Proc. Natl. Acad. Sci. U. S. A. **85:**5122–5125.
23. **Freeman, T. C., et al.** 2007. Construction, visualisation, and clustering of transcription networks from microarray expression data. PLoS Comput. Biol. **3:**e206.
24. **Friedman, R. L., S. P. Manly, M. McMahon, I. M. Kerr, and G. R. Stark.** 1984. Transcriptional and posttranscriptional regulation of interferon-induced gene expression in human cells. Cell **38:**745–755.
25. **Gough, D. J., et al.** 2010. Functional crosstalk between type I and II interferon through the regulated expression of STAT1. PLoS Biol. **8:**e1000361.
26. **Gribaudo, G., et al.** 1993. Interferons inhibit onset of murine cytomegalovirus immediate-early gene transcription. Virology **197:**303–311.
27. **Gribaudo, G., et al.** 1995. Interferon-a inhibits the murine cytomegalovirus

immediate-early gene expression by down-regulating NF-kB activity. Virology **211:**251–260.
28. **Gustems, M., et al.** 2006. Regulation of the transcription and replication cycle of human cytomegalovirus is insensitive to genetic elimination of the cognate NF-{kappa}B binding sites in the enhancer. J. Virol. **80:**9899–9904.
29. **Hanson, L. K., and A. E. Campbell.** 2006. Determinants of macrophage tropism, p. 419–443. *In* M. J. Reddehase and N. Lemmermann (ed.), Cytomegaloviruses: molecular biology and immunology. Caister Academic Press, Norfolk, England.
30. **Heise, M. T., and H. W. Virgin.** 1995. The T-cell-independent role of gamma interferon and tumor necrosis factor alpha in macrophage activation during murine cytomegalovirus and herpes simplex virus infections. J. Virol. **69:**904–909.
31. **Hengel, H., P. Lucin, S. Jonjic, T. Ruppert, and U. H. Koszinowski.** 1994. Restoration of cytomegalovirus antigen presentation by gamma interferon combats viral escape. J. Virol. **68:**289–297.
32. **Holtappels, R., V. Boehm, J. Podlech, and M. Reddehase.** 2008. CD8 T-cell-based immunotherapy of cytomegalovirus infection: proof of concept provided by the murine model. Med. Microbiol. Immunol. **197:**125–134.
33. **Holzinger, D., et al.** 2007. Induction of MxA gene expression by influenza A virus requires type I or type III interferon signaling. J. Virol. **81:**7776–7785.
34. **Honda, K., A. Takaoka, and T. Taniguchi.** 2006. Type I interferon gene induction by the interferon regulatory factor family of transcription factors. Immunity **25:**349–360.
35. **Hummel, M., et al.** 2001. Allogeneic transplantation induces expression of cytomegalovirus immediate-early genes in vivo: a model for reactivation from latency. J. Virol. **75:**4814–4822.
36. **Irizarry, R. A., et al.** 2003. Exploration, normalization, and summaries of high density oligonucleotide array probe level data. Biostatistics **4:**249–264.
37. **Jenner, R. G., and R. A. Young.** 2005. Insights into host responses against pathogens from transcriptional profiling. Nat. Rev. Microbiol. **3:**281–294.
38. **Kalvakolanu, D. V.** 2003. Alternate interferon signaling pathways. Pharmacol. Ther. **100:**1–29.
39. **Karaghiosoff, M., et al.** 2000. Partial impairment of cytokine responses in Tyk2-deficient mice. Immunity **13:**549–560.
40. **Katze, M. G., Y. He, and M. Gale.** 2002. Viruses and interferon: a fight for supremacy. Nat. Rev. Immunol. **2:**675–687.
41. **Kerr, I. M., and G. R. Stark.** 1992. The antiviral effects of the interferons and their inhibition. J. Interferon Res. **12:**237–240.
42. **Kotenko, S. V., et al.** 2003. IFN-[lambda]s mediate antiviral protection through a distinct class II cytokine receptor complex. Nat. Immunol. **4:**69–77.
43. **Kropp, K. A., et al.** 2009. Synergism between the components of the bipartite major immediate-early transcriptional enhancer of murine cytomegalovirus does not accelerate virus replication in cell culture and host tissues. J. Gen. Virol. **90:**2395–2401.
44. **Lacaze, P., et al.** 2009. Combined genome-wide expression profiling and targeted RNA interference in primary mouse macrophages reveals perturbation of transcriptional networks associated with interferon signalling. BMC Genomics **10:**372.
45. **Landolfo, S., G. Gribaudo, A. Angeretti, and M. Gariglio.** 1995. Mechanisms of viral inhibition by interferons. Pharmacol. Ther. **65:**415–442.
46. **Lecellier, C. H., et al.** 2005. A cellular microRNA mediates antiviral defense in human cells. Science **308:**557–560.
47. **Lemmermann, N. A. W., et al.** 2010. CD8 T-cell immunotherapy of cytomegalovirus disease in the murine model, p. 369–420. *In* S. Kaufmann and D. Kabelitz (ed.), Methods in microbiology and immunology of infection, vol. 25. Academic Press, New York, NY.
48. **Liu, H., H. Kang, R. Liu, X. Chen, and K. Zhao.** 2002. Maximal induction of a subset of interferon target genes requires the chromatin-remodeling activity of the BAF complex. Mol. Cell. Biol. **22:**6471–6479.
49. **Livet, J., et al.** 2007. Transgenic strategies for combinatorial expression of fluorescent proteins in the nervous system. Nature **450:**56–62.
50. **Lucin, P., et al.** 1994. Late phase inhibition of murine cytomegalovirus replication by synergistic action of interferon-gamma and tumour necrosis factor. J. Gen. Virol. **75:**101–110.
51. **Mangeat, B., et al.** 2003. Broad antiretroviral defence by human APOBEC3G through lethal editing of nascent reverse transcripts. Nature **424:**99–103.
52. **Matsumoto, M., et al.** 1999. Activation of the transcription factor ISGF3 by interferon-gamma. Biol. Chem. **380:**699–703.
53. **Messerle, M., B. Buhler, G. M. Keil, and U. H. Koszinowski.** 1992. Structural organization, expression, and functional characterization of the murine cytomegalovirus immediate-early gene 3. J. Virol. **66:**27–36.
54. **Messerle, M., I. Crnkovic, W. Hammerschmidt, H. Ziegler, and U. H. Koszinowski.** 1997. Cloning and mutagenesis of a herpesvirus genome as an infectious bacterial artificial chromosome. Proc. Natl. Acad. Sci. U. S. A. **94:**14759–14763.
55. **Min, W., J. S. Pober, and D. R. Johnson.** 1998. Interferon induction of TAP1: the phosphatase SHP-1 regulates crossover between the IFN-alpha and the IFN-gamma signal-transduction pathways. Circ. Res. **83:**815–823.
56. **Orange, J. S., B. Wang, C. Terhorst, and C. A. Biron.** 1995. Requirement for natural killer cell-produced interferon gamma in defense against murine cytomegalovirus infection and enhancement of this defense pathway by interleukin 12 administration. J. Exp. Med. **182:**1045–1065.
57. **Plachter, B., C. Sinzger, and G. Jahn.** 1996. Cell types involved in replication and distribution of human cytomegalovirus. Adv. Virus Res. **46:**195–261.
58. **Podlech, J., R. Holtappels, N. K. A. Grzimek, and M. J. Reddehase.** 2002. Animal models: murine cytomegalovirus, p. 493–525. *In* S. H. E. Kaufmann and D. Kabelitz (ed.), Methods in microbiology, vol. 32. Academic Press, San Diego, CA.
59. **Podlech, J., et al.** 2010. Enhancerless cytomegalovirus is capable of establishing a low-level maintenance infection in severely immunodeficient host tissues but fails in exponential growth. J. Virol. **84:**6254–6261.
60. **Presti, R. M., et al.** 1998. Interferon-gamma regulates acute and latent murine cytomegalovirus infection and chronic disease of the great vessels. J. Exp. Med. **188:**577–588.
61. **Presti, R. M., D. L. Popkin, M. Connick, S. Paetzold, and H. W. Virgin.** 2001. Novel cell type-specific antiviral mechanism of interferon-gamma action in macrophages. J. Exp. Med. **193:**483–496.
62. **R Development Core Team.** 2011. R: a language and environment for statistical computing. R Foundation for Statistical Computing, Vienna, Austria. http://www.R-project.org.
63. **Sadler, A. J., and B. R. G. Williams.** 2008. Interferon-inducible antiviral effectors. Nat. Rev. Immunol. **8:**559–568.
64. **Samarajiwa, S. A., S. Forster, K. Auchettl, and P. J. Hertzog.** 2009. INTERFEROME: the database of interferon regulated genes. Nucleic Acids Res. **37:**D852–D857.
65. **Sarnow, P., C. L. Jopling, K. L. Norman, S. Schuetz, and K. A. Wehner.** 2006. MicroRNAs: expression, avoidance and subversion by vertebrate viruses. Nat. Rev. Microbiol. **4:**651–659.
66. **Schlaak, J. F., et al.** 2002. Cell-type and donor-specific transcriptional responses to interferon-alpha. J. Biol. Chem. **277:**49428–49437.
67. **Schroder, K., P. J. Hertzog, T. Ravasi, and D. A. Hume.** 2004. Interferon-gamma: an overview of signals, mechanisms and functions. J. Leukoc. Biol. **75:**163–189.
68. **Sen, G. C.** 2001. Viruses and interferons. Annu. Rev. Microbiol. **55:**255–281.
69. **Sinzger, C., et al.** 1995. Fibroblasts, epithelial cells, endothelial cells and smooth muscle cells are major targets of human cytomegalovirus infection in-vivo. J. Gen. Virol. **76:**741–750.
70. **Smith, M. G.** 1954. Propagation of salivary gland virus of the mouse in tissue cultures. Proc. Soc. Exp. Biol. Med. **86:**435–440.
71. **Smyth, G. K.** 2004. Linear models and empirical Bayes methods for assessing differential expression in microarray experiments. Stat. Appl. Genet. Mol. Biol. **3:**article 3.
72. **Sommereyns, C., S. Paul, P. Staeheli, and T. Michiels.** 2008. IFN-lambda is expressed in a tissue-dependent fashion and primarily acts on epithelial cells in vivo. PLoS Pathog. 4:e1000017.
73. **Staeheli, P.** 1990. Interferon-induced proteins and the antiviral state. Adv. Virus Res. **38:**147–200.
74. **Stark, G. R., I. M. Kerr, B. R. G. Williams, R. H. Silverman, and R. D. Schreiber.** 1998. How cells respond to interferons. Annu. Rev. Biochem. **67:**227–264.
75. **Stockinger, S., et al.** 2002. Production of type I IFN sensitizes macrophages to cell death induced by Listeria monocytogenes. J. Immunol. **169:**6522–6529.
76. **Strobl, B., et al.** 2005. Novel functions of tyrosine kinase 2 in the antiviral defense against murine cytomegalovirus. J. Immunol. **175:**4000–4008.
77. **Takaoka, A., et al.** 2000. Cross talk between interferon-gamma and -alpha/beta signaling components in caveolar membrane domains. Science **288:**2357–2360.
78. **Takaoka, A., and H. Yanai.** 2006. Interferon signalling network in innate defence. Cell. Microbiol. **8:**907–922.
79. **Taniguchi, T., and A. Takaoka.** 2001. A weak signal for strong responses: interferon-alpha/beta revisited. Nat. Rev. Mol. Cell Biol. **2:**378–386.
80. **Verhaegent, M., and T. K. Christopoulos.** 2002. Recombinant Gaussia luciferase. Overexpression, purification, and analytical application of a bioluminescent reporter for DNA hybridization. Anal. Chem. **74:**4378–4385.
81. **Wagner, M., U. H. Koszinowski, and M. Messerle.** 1999. Systematic excision of vector sequences from the BAC-cloned herpesvirus genome during virus reconstitution. J. Virol. **73:**7056–7060.
82. **Wurdinger, T., et al.** 2008. A secreted luciferase for ex vivo monitoring of in vivo processes. Nat. Methods **5:**171–173.
83. **Zhou, A., et al.** 1995. Exogenous interferon-gamma induces endogenous synthesis of interferon-alpha and -beta by murine macrophages for induction of nitric oxide synthase. J. Interferon Cytokine Res. **15:**897–904.
84. **Zhou, Z., et al.** 2007. Type III Interferon (IFN) Induces a Type I IFN-Like Response in a Restricted Subset of Cells through Signaling Pathways Involving both the Jak-STAT Pathway and the Mitogen-Activated Protein Kinases. J. Virol. **81:**7749–7758.
85. **Zimmermann, A., et al.** 2005. A cytomegaloviral protein reveals a dual role for STAT2 in IFN-{gamma} signaling and antiviral responses. J. Exp. Med. **201:**1543–1553.